Applied Catalysis B: Environmental 232 (2018) 49–54

Contents lists available at ScienceDirect

Applied Catalysis B: Environmental

journal homepage: www.elsevier.com/locate/apcatb

Improved visible-light activity of nitrogen-doped layered niobate photocatalysts by NH_3-nitridation with KCl flux

Hajime Suzuki[a], Osamu Tomita[a], Masanobu Higashi[a], Akinobu Nakada[a], Ryu Abe[a,b,*]

[a] Department of Energy and Hydrocarbon Chemistry, Graduate School of Engineering, Kyoto University, Nishikyo-ku, Kyoto, 615-8510, Japan
[b] JST-CREST, Japan Science and Technology Agency (JST), Kawaguchi, Saitama 332-0012, Japan

ARTICLE INFO

Keywords:
Nitrogen doping
Layered metal oxide
Visible light
Photocatalyst
Flux

ABSTRACT

In the present study, nitrogen doping into layered perovskite niobites, $KCa_2Na_{n-3}Nb_nO_{3n+1}$ (n = 3 or 4), was attempted to enhance their response to visible light during photocatalytic water reduction and oxidation. Although conventional nitridation, i.e., heating in NH_3 stream at a high temperature, produced black-colored samples due to the undesirable reduction of Nb^{5+} to Nb^{4+} (and/or Nb^{3+}), the use of KCl flux with NH_3 stream effectively prevented the reduction of Nb^{5+}, resulting in yellow-colored samples that had a much lower concentration of reduced Nb species. The samples prepared with KCl flux exhibited stronger absorption (at λ = 350–550 nm) when compared to those prepared without KCl flux. This was due to the higher concentration of N^{3-} anions, as confirmed by elemental analysis and the observed peak shift in XRD patterns. On the other hand, the absorption band with λ > 550 nm, which indicated the presence of reduced species or anion vacancies, were astonishingly smaller for the samples prepared with KCl than for those without KCl. This indicated that the formation of reduced Nb species was inhibited by KCl. XPS analysis also supported this effect. The use of KCl flux also prevented the problematic decrease in the concentration of potassium cations in the interlayer space during high-temperature treatment in NH_3 flow. The samples prepared with KCl flux exhibited much higher O_2 and H_2 evolution rates under visible-light irradiation in the presence of an electron acceptor and a donor, respectively as compared to those prepared without KCl. This clear improvement in O_2 and H_2 evolution was probably due to the larger amount of doped nitrogen introduced and/or the suppressed formation of reduced Nb species.

1. Introduction

Cation-exchangeable layered metal oxides, such as $K_4Nb_6O_{17}$, have been studied as promising photocatalytic materials for water splitting [1–12]. They consist of two-dimensional anionic sheets of oxide and alkali metal cations that electrostatically interact to form a well-ordered layered structure. Indeed, some cation-exchangeable layered metal oxides, such as $K_4Nb_6O_{17}$, $K_2La_2Ti_3O_{10}$, $RbNdTa_2O_7$, and $NaCa_2Ta_3O_{10}$, have been reported as efficient photocatalysts for water splitting under UV irradiation [1–4]. The nanosheets prepared by exfoliation of these layered materials have also been extensively studied to enhance photocatalytic activity [13,14]. However, such cation-exchangeable layered metal oxides generally possess wide bandgaps, and thus, are responsive only to UV light. It is essential to utilize visible light for practical H_2 production since nearly half of the solar energy incident on Earth's surface lies in the visible region (400 < λ < 800 nm).

Nitrogen doping into oxide semiconductors is a highly active research area, in order to enable them to absorb visible light. Among nitrogen-doped materials, N-doped TiO_2 has been studied for a wide variety of applications, including decomposition of organic pollutants and solar energy conversion (*i.e.*, water splitting) [15–23]. Although nitrogen doping into simple oxides has been widely studied, reports on that into layered metal oxides are sparse. For example, nitrogen doping into layered tantalates and titanates (e.g., $CsCa_2Ta_3O_{10}$, $RbLaTa_2O_7$ and $Cs_{0.68}Ti_{1.83}O_4$) led to a color change from white to yellow or orange [24–26], which enabled them to absorb and utilize visible light during photocatalysis. On the other hand, effective N-doping into a layered niobium(V) oxide is still challenging due to undesirable reduction of Nb^{5+} cation during N-doping process. For example, high-temperature NH_3-nitridation process on a layered niobate $KCa_2Nb_3O_{10}$ produced a black-colored sample, which was different from the general trend in Ta- or Ti-based ones, and indicated that a significant fraction of Nb^{5+} was reduced to Nb^{4+} (and/or Nb^{3+}) under the reductive atmosphere of NH_3 [27]. Similar reduction of Nb^{5+} has been reported to occur during the synthesis of non-layered niobium (oxy)nitrides, such as $BaNbO_2N$ [28]. Generally, the extensive formation of such reduced species lowers the

* Corresponding author at: Department of Energy and Hydrocarbon Chemistry, Graduate School of Engineering, Kyoto University, Nishikyo-ku, Kyoto, 615-8510, Japan.
E-mail address: ryu-abe@scl.kyoto-u.ac.jp (R. Abe).

https://doi.org/10.1016/j.apcatb.2018.03.007
Received 19 December 2017; Received in revised form 27 February 2018; Accepted 1 March 2018
Available online 08 March 2018
0926-3373/

photocatalytic activity due to the species acting as the recombination center. Thus, preventing the reduction of Nb^{5+} during high-temperature NH_3-treatment is crucial for obtaining highly active N-doped niobium oxide based photocatalysts. In addition, we have recently reported that high-temperature NH_3-treatment of layered metal oxides decreases the concentration of alkaline metal cations in the interlayer spaces, which leads to the formation of impurities or destruction of layered structures [25]. Preventing the depletion of alkaline metal cations, therefore, is important as it helps in retaining and taking advantage of the original features of layered materials.

In the present study, we have demonstrated that the use of KCl flux during high-temperature NH_3-treatment of layered perovskite niobates $KCa_2Na_{n-3}Nb_nO_{3n+1}$ (n = 3 or 4) helps in inhibiting both the decrease in the number of potassium cations and the reduction of Nb^{5+}, and thereby, enables higher photocatalytic activities for water oxidation and reduction under visible-light irradiation as compared to those prepared by conventional NH_3-treatment (i.e., without KCl).

2. Experimental Section

2.1. Catalyst preparation

Particles of $KCa_2Na_{n-3}Nb_nO_{3n+1}$, where n = 3 or 4 (see Fig. 1 for their crystal structures), were prepared by a solid-state reaction [29,30]. $KCa_2Nb_3O_{10}$ was prepared via calcination of a mixture of K_2CO_3, $CaCO_3$, and Nb_2O_5 (K:Ca:Nb = 1.1: 2:3) in air at 1473 K for 12 h. Here K_2CO_3 was present at 1.1-fold the stoichiometric value to compensate for the volatilization of potassium during the high-temperature synthesis. For the preparation of $KCa_2NaNb_4O_{13}$, $NaNbO_3$ particles were first synthesized by calcining a mixture of Na_2CO_3 and Nb_2O_5 (Na:Nb = 1.1:1) at 1173 K for 10 h, then mixed with $KCa_2Nb_3O_{10}$ in 1:1 molar ratio, and finally calcined at 1473 K for 48 h. The layered metal oxides thus obtained (1 g) were then heated under NH_3 flow (100 mL/min) at 1073 K for 6 h in the absence or presence of KCl (melting point: 1043 K; 50 wt% of the catalysts). As shown in Fig. S1, the impurity peaks were obviously observed in the XRD patterns of $KCa_2Na_{n-3}Nb_nO_{3n+1}$ after nitridation with KCl flux at a higher temperature of 1173 K, indicating the destruction of layers. Therefore, the NH_3 treatments were performed at 1073 K. The samples without and with KCl flux were denoted as $KCa_2Na_{n-3}Nb_nO_{3n+1}$:N and $KCa_2Na_{n-3}Nb_nO_{3n+1}$:N (KCl), respectively.

The K^+ ions in the interlayer spaces of the layered compounds were replaced with H^+ by stirring the particles in 5 M HNO_3 for 72 h. The particles were collected via centrifugation, washed with distilled water, and dried in air at room temperature. The samples thus obtained were denoted as $H^+/KCa_2Na_{n-3}Nb_nO_{3n+1}$, $H^+/KCa_2Na_{n-3}Nb_nO_{3n+1}$:N, and $H^+/KCa_2Na_{n-3}Nb_nO_{3n+1}$:N (KCl).

2.2. Characterization

Sample characterization was carried out by powder-XRD (MiniFlex II, Rigaku Corp., Cu Kα), UV-visible diffuse reflectance spectroscopy (UV-vis, V-670, JASCO Corp., reference sample: $BaSO_4$), scanning electron microscopy (SEM, VE-9800, KEYENCE Corp.), thermogravimetric and differential thermal analysis (TG-DTA, Thermo plus evo2, Rigaku Corp.), and energy dispersive X-ray spectrometry (EDX, INCA x-act, Oxford instruments). X-ray photoelectron spectroscopy (XPS) measurements were performed using an ULVAC-PHI 5500MT system. The binding energies were referenced to the C1s level (284.8 eV). Elemental analysis was performed by inductively coupled plasma atomic emission spectroscopy (ICP-AES, iCAP 7400 Duo, Thermo Fisher Scientific Inc.). Particles of the layered compounds (50 mg) were dissolved in a mixture of HF (1 mL), HNO_3 (3 mL), and H_2SO_4 (15 mL) using a Teflon beaker. Tartaric acid (0.5 g) was added to the solution to prevent hydrolysis of niobium. Then, this solution was transferred to a volumetric flask with H_2O_2 (30%, 1 mL) and diluted to 100 mL with distilled water.

2.3. Photocatalytic reactions

Photocatalytic reactions were conducted in a Pyrex glass reactor connected to a closed gas-circulation system. Photocatalyst powder (100 mg) was suspended in the magnetically stirred reactor using 70 mL of an aqueous $AgNO_3$ solution containing $Co(NO_3)_3$ (0.5 wt% of Co to the photocatalyst) or using an aqueous MeOH solution (10 vol%) containing H_2PtCl_6 (0.5 wt% of Pt to the photocatalyst). $Co(OH)_x$ and Pt, which served as O_2 and H_2 evolution co-catalysts, respectively, were deposited on the photocatalysts in the reactor. These suspensions were thoroughly degassed, and then irradiated using a 300 W Xe lamp, which was equipped with a cutoff filter (λ > 400 nm). The gases thus produced were analyzed using online gas chromatography (TCD; molecular sieve 5A; Ar carrier).

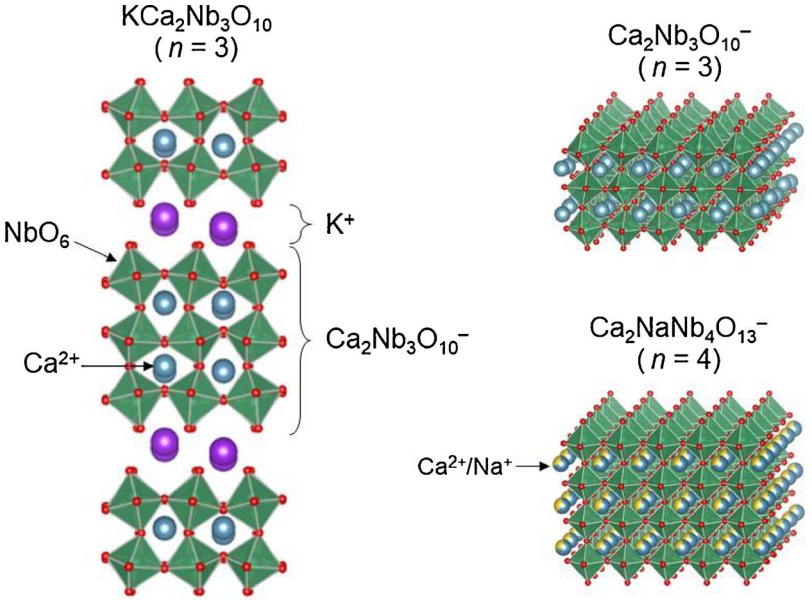

Fig. 1. Structural model of $KCa_2Na_{n-3}Nb_nO_{3n+1}$.

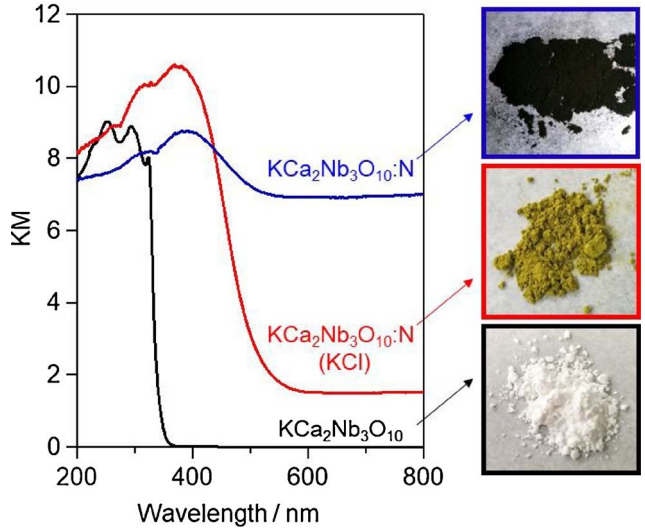

Fig. 2. Diffuse reflectance spectra and physical appearance of $KCa_2Nb_3O_{10}$ and the nitrided sample, with or without KCl.

3. Results and Discussion

3.1. Characterization of N-doped $KCa_2Na_{n-3}Nb_nO_{3n+1}$ samples

Fig. 1 shows a structural model of $KCa_2Na_{n-3}Nb_nO_{3n+1}$ [31–33]. It consists of two-dimensional anionic sheets (*i.e.*, perovskite layers) of niobate and alkali metal cations that electrostatically interact to form a well-ordered and cation-exchangeable layered structure. In this series, the perovskite-slab thickness was determined by the number of stacked NbO_6 octahedra along stacking distance, *n*. Figs. 2 and 3 show diffuse reflectance spectra of $KCa_2Nb_3O_{10}$ and $KCa_2NaNb_4O_{13}$, respectively, before and after NH_3-treatment at 1073 K, along with their photographs. The original $KCa_2Nb_3O_{10}$ and $KCa_2NaNb_4O_{13}$ samples showed an absorption band below 350 nm, which resulted in their white color. Heating in NH_3 led to significant change in the absorption and in the sample colors (yellow or black). The sample color was dependent on whether the KCl flux was used during the NH_3 heating conditions. The samples after NH_3-treatment exhibited two new absorptions: one at λ = 350-550 nm and the other at λ > 550 nm. The former was due to the incorporation of N^{3-} anions in the layered structure, which enabled visible-light excitation from the N 2p orbital to the conduction band.

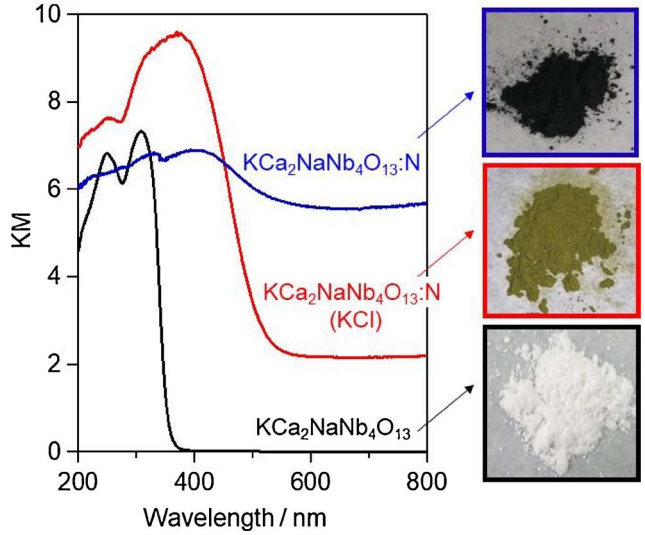

Fig. 3. Diffuse reflectance spectra and physical appearance of $KCa_2NaNb_4O_{13}$ and the nitrided sample, with or without KCl.

This absorption is commonly observed for nitrogen-doped metal oxides (e.g. N-doped TiO_2). The latter background absorption band, above 550 nm, was attributed to the presence of reduced Nb species, such as Nb^{4+} (or Nb^{3+}), and/or anion vacancies. Clearly, the presence of KCl flux significantly affected these two absorptions. In both cases of $KCa_2Nb_3O_{10}$ and $KCa_2NaNb_4O_{13}$ samples, the former absorption band (~ 550 nm) derived from N^{3-} insertion was increased by the use of KCl flux. On the other hand, the latter absorption was drastically decreased in the presence of KCl flux. These findings strongly suggested that the use of KCl flux in NH_3-nitridation increases the number of N^{3-} anions in the crystal-lattice and decreases the extent of the undesirable reduction of Nb^{5+}. The nitrogen content of $KCa_2Nb_3O_{10}$:N, $KCa_2Nb_3O_{10}$:N (KCl), $KCa_2NaNb_4O_{13}$:N, and $KCa_2NaNb_4O_{13}$:N (KCl) was determined to be 0.9, 1.5, 0.8, and 2.0 wt%, respectively, by HNO analysis, confirming that the amount of N^{3-} introduced was indeed increased by the use of KCl flux. Although the precise molar amount of oxygen could not be determined via this analysis, three oxygen atoms will be substituted by two nitrogen atoms to compensate the charge by considering the valences of O^{2-} and N^{3-}. Thus, the composition of $KCa_2Nb_3O_{10}$:N, $KCa_2Nb_3O_{10}$:N (KCl), $KCa_2NaNb_4O_{13}$:N, and $KCa_2NaNb_4O_{13}$:N (KCl) can be plausibly expressed by the formula of $KCa_2Nb_3O_{9.55}N_{0.3}$, $KCa_2Nb_3O_{9.1}N_{0.6}$, $KCa_2NaNb_4O_{12.4}N_{0.4}$, and $KCa_2NaNb_4O_{11.5}N_{1.0}$. As shown in Fig. S2, the N 1s peaks for $KCa_2Nb_3O_{10}$:N (KCl) and $KCa_2NaNb_4O_{13}$:N (KCl) were observed at 395.3 and 395.5 eV, respectively, which can be assigned to N^{3-} in the lattice. The peak position was close to that of oxynitrides, such as $SrNbO_2N$ [34]. Peaks associated with surface-adsorbed nitrogen species [15,35] and ammonium ions [36], which are typically located around 399 ~ 402 eV, were not observed. This XPS result confirms that nitrogen was incorporated in the niobate layers as N^{3-}. Fig. 4 shows XP spectra of the Nb 3d region for these samples. For both $KCa_2Nb_3O_{10}$ and $KCa_2NaNb_4O_{13}$, the Nb $3d_{5/2}$ and $3d_{3/2}$ peaks are observed at *ca.* 206.5 and 209.3 eV, respectively, which are commonly attributed to the oxidation state of Nb^{5+}. Although there was a broad peak around 203.2 eV, which emerged after NH_3-treatment and is associated with reduced Nb species, the peak intensities drastically decreased by the use of KCl flux. The XPS results appear to concur with the results deduced from the UV-vis spectra (see Figs. 2 and 3).

Note that the original crystal structure of $KCa_2Nb_3O_{10}$ and $KCa_2NaNb_4O_{13}$ were mostly maintained even after NH_3-nitridation at 1073 K, as confirmed by XRD measurements (see Figs. 5 and 6), in which patterns were almost unaltered, while a slight change in the peak intensities was observed. However, the peak position changed after the NH_3-treatment, for example, shown in the extended part around 2θ = 23° for (100) and (010) of $KCa_2Nb_3O_{10}$ and $KCa_2NaNb_4O_{13}$, respectively. This variation was different depending on whether samples were prepared with or without KCl flux. The positions of these peaks were shifted to a lower value when NH_3-treatment was performed with KCl. Such a large shift strongly suggests that many oxygen anions (O^{2-}) were substituted by nitrogen anions (N^{3-}) that have a larger ionic radius.

The XRD measurements showed that the original layered structures of these sample were almost maintained. However, we noticed that the amount of potassium in the NH_3-treated samples was significantly affected by the presence or absence of KCl flux. Table 1 shows the molar ratio of K to Nb in $KCa_2Nb_3O_{10}$, $KCa_2NaNb_4O_{13}$, and the N-doped samples, which was determined by EDX and ICP. The K/Nb values obviously decreased after NH_3-treatment without KCl, which is in accordance with the previously reported NH_3-treatment of $RbLaTa_2O_7$ [25]. In marked contrast, the K/Nb ratios did not decrease after NH_3-treatment in the presence of KCl. These elemental analyses indicate that applying KCl flux not only prevents the undesirable reduction of Nb^{5+}, but also effectively decreases volatilization of potassium cations during heating in NH_3. It should be note that the chlorine content in $KCa_2Nb_3O_{10}$:N (KCl) and $KCa_2NaNb_4O_{13}$:N (KCl) was negligible. Fig. 7 shows SEM images of $KCa_2Nb_3O_{10}$ and $KCa_2NaNb_4O_{13}$, and the nitrogen-doped versions of those samples. Images of original layered

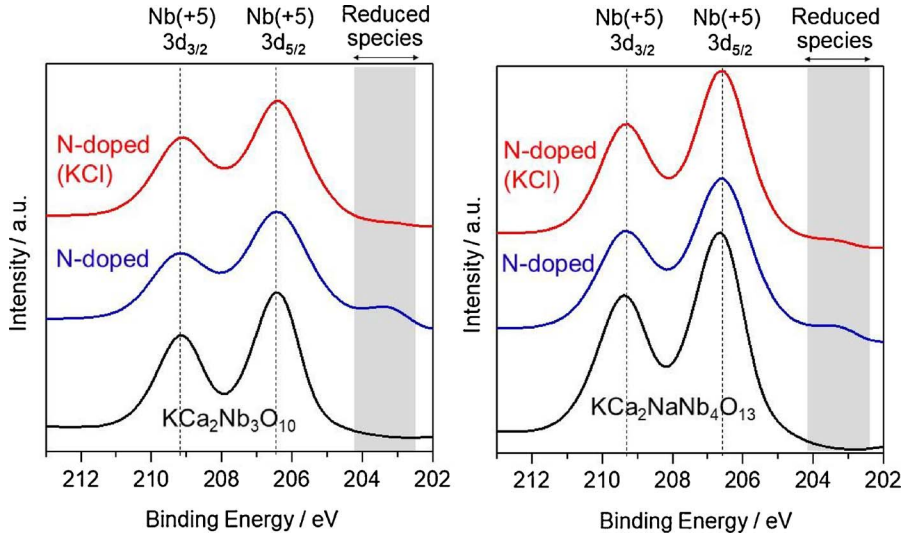

Fig. 4. X-ray photoelectron spectra of Nb 3d region for $KCa_2Nb_3O_{10}$, $KCa_2NaNb_4O_{13}$, and the nitrided samples, with or without KCl.

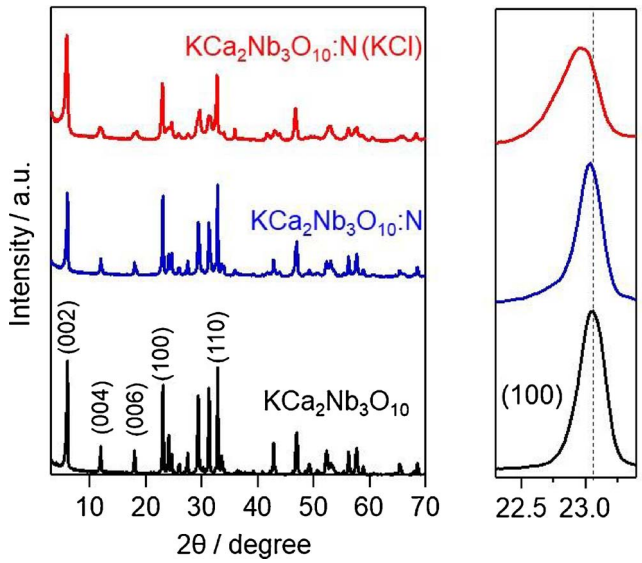

Fig. 5. XRD patterns of $KCa_2Nb_3O_{10}$ and the nitrided sample, with or without KCl.

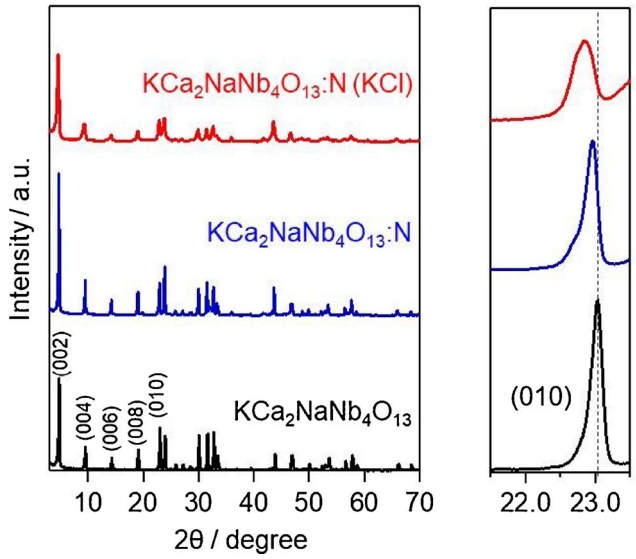

Fig. 6. XRD patterns of $KCa_2NaNb_4O_{13}$ and the nitrided sample, with or without KCl.

Table 1
K/Nb ratio of $KCa_2Nb_3O_{10}$, $KCa_2NaNb_4O_{13}$, and the nitrided samples, with or without KCl.

Sample	K/Nb ratio	
	EDX	ICP
$KCa_2Nb_3O_{10}$	0.32	0.38
$KCa_2Nb_3O_{10}$:N	0.25	0.29
$KCa_2Nb_3O_{10}$:N (KCl)	0.37	0.38
$KCa_2NaNb_4O_{13}$	0.23	–
$KCa_2NaNb_4O_{13}$:N	0.18	–
$KCa_2NaNb_4O_{13}$:N (KCl)	0.24	–

– not measured.

metal oxides, $KCa_2Nb_3O_{10}$ and $KCa_2NaNb_4O_{13}$, exhibit an aggregation of plate-like primary particles with grain sizes of several micrometers. Although the shape and morphology of $KCa_2Nb_3O_{10}$ remained intact after NH_3-treatment in the absence of KCl, the same cannot be said of samples that were prepared with KCl, which suggests that particles of $KCa_2Nb_3O_{10}$:N (KCl) and $KCa_2NaNb_4O_{13}$:N (KCl) were produced, at least partially, via dissolution-reprecipitation process afforded by KCl solution.

3.2. Photocatalytic water oxidation and reduction over N-doped samples

Fig. 8 shows the time courses of O_2 evolution from water over photocatalyst samples under visible-light irradiation in the presence of Ag^+ (as an electron acceptor). Before each reaction, a small amount of $Co(NO_3)_3$ was added to form $Co(OH)_x$ co-catalysts that could enhance water oxidation.[37] Both the original samples, $KCa_2Nb_3O_{10}$ and $KCa_2NaNb_4O_{13}$, show no activity for O_2 evolution due to their insensitivity to visible light. Although it has recently been reported that $Co(OH)_x$ functions as a visible-light absorption center on TiO_2,[38] the absence of O_2 evolution during the reaction involving $Co(OH)_x$-loaded samples indicates that such visible-light absorption by $Co(OH)_x$ can be safely ignored under the present reaction conditions. On the other hand, N-doped samples were seen to generate appreciable amount of O_2 under visible-light irradiation. Importantly, the samples prepared with KCl flux (i.e., $KCa_2Nb_3O_{10}$:N (KCl) and $KCa_2NaNb_4O_{13}$:N (KCl), as shown by red symbols) exhibited about 3-to-4 times higher O_2 evolution rate than those prepared without KCl (i.e., $KCa_2Nb_3O_{10}$:N and $KCa_2NaNb_4O_{13}$, as shown as blue symbols). This clear improvement in O_2 evolution is probably due to a higher concentration of nitrogen and/or the depletion of reduced Nb species. Fig. S3 shows the evolution of

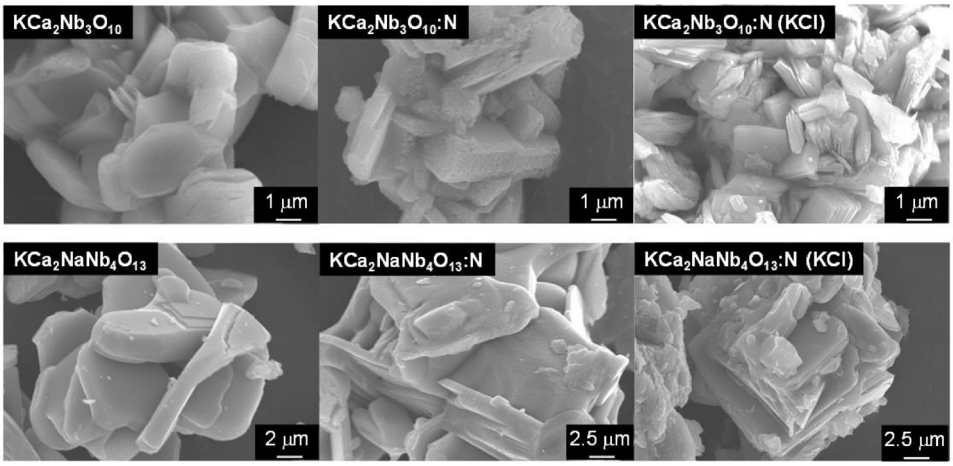

Fig. 7. SEM images of $KCa_2Nb_3O_{10}$, $KCa_2NaNb_4O_{13}$, and the nitrided samples, with or without KCl.

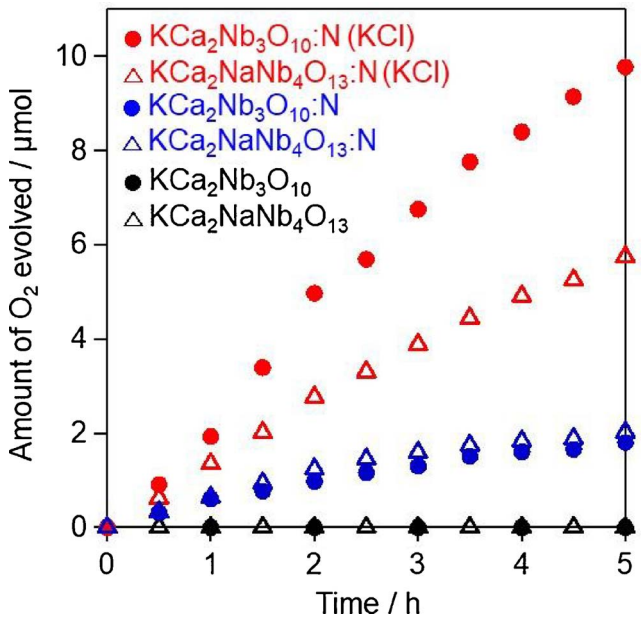

Fig. 8. O_2 evolution under visible-light irradiation ($\lambda > 400$ nm) over $KCa_2Nb_3O_{10}$, $KCa_2NaNb_4O_{13}$, and the nitrided samples, with or without KCl, in aqueous $AgNO_3$ solution (10 mM, 70 mL) containing $Co(NO_3)_3$ (0.5 wt% of Co to the photocatalyst).

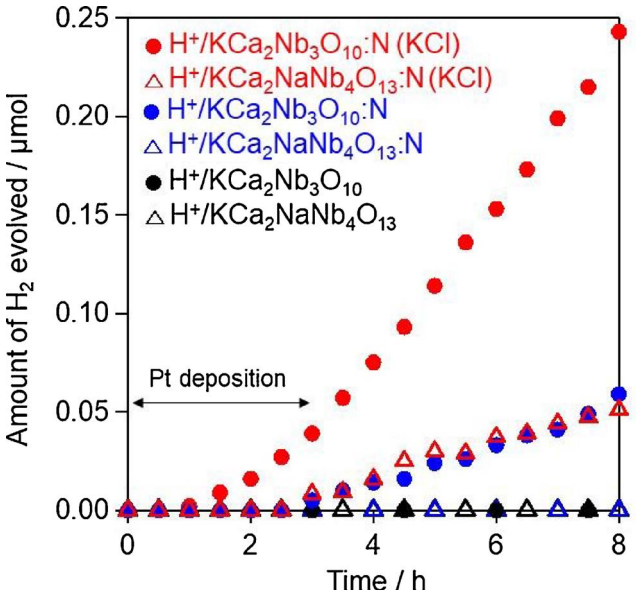

Fig. 9. H_2 evolution over $H^+/KCa_2Nb_3O_{10}$, $H^+/KCa_2NaNb_4O_{13}$, and the nitrided samples, with or without KCl, in aqueous MeOH solution (10 vol%, 70 mL) containing H_2PtCl_6 (0.5 wt% of Pt to the photocatalyst) under visible-light irradiation ($\lambda > 400$ nm).

O_2 over $KCa_2Nb_3O_{10}$:N (KCl) and $KCa_2NaNb_4O_{13}$:N (KCl) in aqueous $AgNO_3$ solution under irradiation from a Xe lamp fitted with different cut-off filters. The onset of O_2 evolution was at ca. 520 nm, which is consistent with their absorption spectra. The O_2 evolution rate increases drastically with a decrease in the cut-off wavelength. This result clearly indicated that the evolution of O_2 took place photocatalytically by the band-gap excitation of the nitrogen-doped layered niobate photocatalysts.

Fig. 9 shows H_2 evolution over proton-exchanged photocatalyst samples in the presence of methanol (MeOH) as an electron donor. $H^+/KCa_2Nb_3O_{10}$:N (KCl) showed about 4 times higher H_2 evolution rate than $H^+/KCa_2Nb_3O_{10}$:N, probably due to the same reason why $KCa_2Nb_3O_{10}$:N (KCl) exhibited higher O_2 evolution rate than $KCa_2Nb_3O_{10}$:N. The observed induction period (~3 h) is attributed to the photocatalytic reduction of Pt^{4+} precursor to metallic Pt°, which functions as a H_2 evolution co-catalyst. Applying KCl flux also improved the rate of photocatalytic H_2 evolution over N-doped $H^+/KCa_2NaNb_4O_{13}$. However, $H^+/KCa_2NaNb_4O_{13}$:N (KCl) showed much lower H_2 evolution rate than $H^+/KCa_2Nb_3O_{10}$:N (KCl). One of the most likely reasons for the low H_2 evolution rate of $H^+/KCa_2NaNb_4O_{13}$:N (KCl) is the lower conduction band level of $H^+/KCa_2NaNb_4O_{13}$ compared to $H^+/KCa_2Nb_3O_{10}$. Fig. S4 shows diffuse reflectance spectra and supposed band positions of $H^+/KCa_2Nb_3O_{10}$ and $H^+/KCa_2NaNb_4O_{13}$. Assuming that the valence band maxima of them were 3 V (vs. NHE), [39] the conduction band minimum (CBM) of $H^+/KCa_2NaNb_4O_{13}$ would be more positive (~0.2 V) than that of $H^+/KCa_2Nb_3O_{10}$. Although the accurate band levels of the materials are unknown, it can be expected that $H^+/KCa_2NaNb_4O_{13}$:N has a lower CBM than that of $H^+/KCa_2Nb_3O_{10}$:N, which leads to a smaller driving force for the reduction of H^+ to H_2 (see Fig. S4).

4. Conclusion

In summary, we demonstrated for the first time that the use of KCl flux in NH_3-treatment is effective for improving the photocatalytic activity of nitrogen-doped layered niobates, i.e., $KCa_2Na_{n-3}Nb_nO_{3n+1}$. The KCl flux played three key roles: (1) mitigating the depletion of potassium cations during heating in NH_3, (2) increasing the amount of doped nitrogen in the lattice, and (3) suppressing the amount of reduced Nb species. Although the photocatalytic activities of $KCa_2Na_{n-3}Nb_nO_{3n+1}$:N (KCl) are still low, improvement in activity can

be achieved by the exfoliation of them to nanosheets. Single-phase niobium(V) (oxy)nitrides and N-doped samples are more difficult to prepare via high-temperature NH_3-treatment, as compared to tantalum (V) samples, due to the facile reduction of Nb^{5+}. The present NH_3-treatment in KCl flux is expected to prevent the undesirable reduction of Nb^{5+} in various niobates, and thereby, enabling us to prepare novel niobium-based (oxy)nitrides. The method can probably be applied to other layered metal oxides where cations are susceptible to reduction, thus opening up the possibility of developing highly active N-doped layered oxide photocatalysts.

Acknowledgments

This work was financially supported by the JST-CREST project, the JSPS KAKENHI Grant Number 17H06439 in Scientific Research on Innovative Areas “Innovations for Light-Energy Conversion (I^4LEC)”, the JSPS Grant-in-Aid for Scientific Research (B) (Grant Number 15H03849), and for JSPS Research Fellow (Grant Number 16J11397). The authors are also indebted to the technical division of Institute for Catalysis, Hokkaido University for their help in building the experimental equipment.

Appendix A. Supplementary data

Supplementary material related to this article can be found, in the online version, at doi:https://doi.org/10.1016/j.apcatb.2018.03.007.

References

[1] K. Domen, A. Kudo, A. Shinozaki, A. Tanaka, K. Maruya, T. Onishi, J. Chem. Soc. Chem. Comm. (1986) 356–357.
[2] T. Takata, K. Shinohara, A. Tanaka, M. Hara, J.N. Kondo, K. Domen, J. Photochem. Photobiol. A 106 (1997) 45–49.
[3] M. Machida, J. Yabunaka, T. Kijima, Chem. Commun. (1999) 1939–1940.
[4] M. Machida, T. Mitsuyama, K. Ikeue, S. Matsushima, M. Arai, J. Phys. Chem. B 109 (2005) 7801–7806.
[5] K. Shimizu, S. Itoh, T. Hatamachi, T. Kodama, M. Sato, K. Toda, Chem. Mater. 17 (2005) 5161–5166.
[6] M. Shibata, A. Kudo, A. Tanaka, K. Domen, K. Maruya, T. Onishi, Chem. Lett. (1987) 1017–1018.
[7] J. Yoshimura, Y. Ebina, J. Kondo, K. Domen, A. Tanaka, J. Phys. Chem. 97 (1993) 1970–1973.
[8] A. Kudo, T. Kondo, J. Mater. Chem. 7 (1997) 777–780.
[9] M.R. Allen, A. Thibert, E.M. Sabio, N.D. Browning, D.S. Larsen, F.E. Osterloh, Chem. Mater. 22 (2010) 1220–1228.
[10] K. Domen, Y. Ebina, T. Sekine, A. Tanaka, J. Kondo, C. Hirose, Catal. Today 16 (1993) 479–486.
[11] K. Sayama, H. Arakawa, K. Domen, Catal. Today 28 (1996) 175–182.
[12] H. Suzuki, O. Tomita, M. Higashi, R. Abe, Catal. Sci. Technol. 5 (2015) 2640–2648.
[13] Y. Ebina, T. Sasaki, M. Harada, M. Watanabe, Chem. Mater. 14 (2002) 4390–4395.
[14] T. Oshima, D.L. Lu, O. Ishitani, K. Maeda, Angew. Chem. Int. Edit 54 (2015) 2698–2702.
[15] R. Asahi, T. Morikawa, T. Ohwaki, K. Aoki, Y. Taga, Science 293 (2001) 269–271.
[16] A. Fujishima, X.T. Zhang, D.A. Tryk, Surf. Sci. Rep. 63 (2008) 515–582.
[17] Y. Cong, J.L. Zhang, F. Chen, M. Anpo, J. Phys. Chem. C 111 (2007) 6976–6982.
[18] X.B. Chen, C. Burda, J. Phys. Chem. B 108 (2004) 15446–15449.
[19] M. Sathish, B. Viswanathan, R.P. Viswanath, C.S. Gopinath, Chem. Mater. 17 (2005) 6349–6353.
[20] G.R. Torres, T. Lindgren, J. Lu, C.G. Granqvist, S.E. Lindquist, J. Phys. Chem. B 108 (2004) 5995–6003.
[21] M. Batzill, E.H. Morales, U. Diebold, Phys. Rev. Lett. (2006) 96.
[22] A. Nakada, S. Nishioka, J.J.M. Vequizo, K. Muraoka, T. Kanazawa, A. Yamakata, S. Nozawa, H. Kumagai, S. Adachi, O. Ishitani, K. Maeda, J. Mater. Chem. A 5 (2017) 11710–11719.
[23] K. Maeda, Y. Shimodaira, B. Lee, K. Teramura, D. Lu, H. Kobayashi, K. Domen, J. Phys. Chem. C 111 (2007) 18264–18270.
[24] S. Ida, Y. Okamoto, M. Matsuka, H. Hagiwara, T. Ishihara, J. Am. Chem. Soc. 134 (2012) 15773–15782.
[25] H. Suzuki, O. Tomita, M. Higashi, R. Abe, J. Mater. Chem. A 4 (2016) 14444–14452.
[26] G. Liu, P. Niu, L.Z. Wang, G.Q. Lu, H.M. Cheng, Catal. Sci. Technol. 1 (2011) 222–225.
[27] S. Ida, Y. Okamoto, S. Koga, H. Hagiwara, T. Ishihara, RSC Adv. 3 (2013) 11521–11524.
[28] M. Kodera, M. Katayama, T. Hisatomi, T. Minegishi, K. Domen, Crystengcomm 18 (2016) 3186–3190.
[29] Y. Ebina, N. Sakai, T. Sasaki, J. Phys. Chem. B 109 (2005) 17212–17216.
[30] Y. Ebina, K. Akatsuka, K. Fukuda, T. Sasaki, Chem. Mater. 24 (2012) 4201–4208.
[31] M. Dion, M. Ganne, M. Tournoux, Mater. Res. Bull. 16 (1981) 1429–1435.
[32] T. Tokumitsu, K. Toda, T. Aoyagi, D. Sakuraba, K. Uematsu, M. Sato, J. Ceram. Soc. Jpn. 114 (2006) 795–797.
[33] A.J. Jacobson, J.W. Johnson, J.T. Lewandowski, Inorg. Chem. 24 (1985) 3727–3729.
[34] K. Maeda, M. Higashi, B. Siritanaratkul, R. Abe, K. Domen, J. Am. Chem. Soc. 133 (2011) 12334–12337.
[35] Y.K. Kim, S. Park, K.J. Kim, B. Kim, J. Phys. Chem. C 115 (2011) 18618–18624.
[36] A.V. Naumkin, A. Kraut-Vass, S.W. Gaarenstroom, C.J. Powell, NIST X-ray Photoelectron Spectroscopy Database, NIST Standard Reference Database 20, Version 4.1, (2018).
[37] G.G. Zhang, S.H. Zang, X.C. Wang, ACS Catal. 5 (2015) 941–947.
[38] K. Maeda, K. Ishimaki, Y. Tokunaga, D.L. Lu, M. Eguchi, Angew. Chem. Int. Edit 55 (2016) 8309–8313.
[39] D.E. Scaife, Sol. Energy 25 (1980) 41–54.